

Copyright © IJCESEN

International Journal of Computational and Experimental Science and ENgineering (IJCESEN)

Vol. 11-No.4 (2025) pp. 8614-8624 http://www.ijcesen.com

ISSN: 2149-9144

Research Article



Sandip Kumar^{1*}, Vineet Shekher², Kaushik Paul³

¹Department of Electrical Engineering, BIT Sindri (under JUT Ranchi), Dhanbad, Jharkhand, India. Corresponding Author Email: sandip.rsee22@bitsindri.ac.in-ORCID: 0000-0002-5247-0050

²Department of Electrical Engineering, GEC Palamu (under JUT Ranchi), Palamu, Jharkhand, India. Email: vineet.ee@bitsindri.ac.in-ORCID: 0000-0002-5200-7850

³Department of Electrical Engineering, BIT Sindri (under JUT Ranchi), Dhanbad, Jharkhand, India. Email: Kaushik.ee@bitsindri.ac.in- ORCID: 0000-0002-5007-7850

Article Info:

DOI: 10.22399/ijcesen.3618 Received: 03 September 2025 Revised: 21 October 2025 Accepted: 28 October 2025

Keywords

Photo Voltaic (PV), Internal Combustion (IC), Electric Vehicle (EV), Renewable Source Modules (RSM), Unified Power Quality Conditioner (UPQC)

Abstract:

In Renewable energy sources, primarily PV plants and wind farms, are increasingly replacing conventional power generation methods. To further reduce environmental pollution, traditional IC engine vehicles are being replaced by zero-emission EVs. The RSMs and charging circuits used in EVs rely on high-power electronic switches, which operate at high switching frequencies. These switching operations, along with rapid variations in power generation, introduce several power quality issues into the grid most notably voltage sags, swells, and harmonics. Such disturbances can damage both grid-connected devices and power sources. To address these challenges, this paper proposes the integration of a UPQC between the grid-connected RSMs and EV charging stations. The UPOC controllers are enhanced using advanced control strategies featuring adaptive and hybrid regulators to ensure optimal power quality. The paper presents a detailed discussion on the proposed system's design and the structure of the various controller regulators. This review explores the application of adaptive and hybrid regulators in UPQC systems to enhance their effectiveness in maintaining optimal PQ. It critically analyses various control methodologies, their adaptability to real-time grid conditions, and their coordination with renewable and EV-based systems. A comparative assessment is provided based on performance metrics such as response time, harmonic mitigation, voltage regulation, and system stability.

1. Introduction

With the global population steadily increasing, the demand for electrical power is rising significantly each day. This growing demand necessitates the expansion of power generation capacity and the extension of the electrical grid to ensure supply reliability. Traditionally, this demand has been met by conventional power generation methods such as coal, diesel, and nuclear plants. However, these contribute heavily to environmental methods pollution [1]–[5], leading to rising global temperatures and creating increasingly uninhabitable conditions for life on Earth. To combat the environmental impact of conventional energy sources, there is a pressing need to transition to renewable energy generation. Renewable energy

plants harness natural resources such as solar radiation, wind, tidal waves, and biogas to produce electricity. However, because these natural resources are inherently variable, the power generated by sources is often unstable renewable unpredictable.Renewable generation systems like PV plants, wind farms, and tidal energy stations typically produce power with fluctuating voltage levels. To stabilize these variations, high-capacity power electronic circuits are employed. These circuits help maintain consistent voltage output despite variable generation conditions [6], [7]. However, the high-frequency switching inherent in these circuits—especially in RSMs—introduces harmonics into the grid. Additionally, rapid changes in load can cause voltage sags and swells, further compromise grid stability and reducing the reliability of connected devices. To further reduce carbon emissions, EVs are being adopted as alternatives to IC engine vehicles. EVs operate using electric motors powered by battery storage systems, which ideally should be charged using renewable energy sources to maintain a zero-emission profile [8]– [12]. Together, the shift to renewable power generation and EV adoption significantly mitigates environmental pollution and promotes more sustainable living conditions globally. However, integrating RSMs and EV charging infrastructure into the grid using high-power electronic components results in increased harmonic distortion and voltage fluctuations. These power quality issues must be addressed to ensure the reliable operation of all grid-connected equipment [13]–[16]. To mitigate these issues, a Unified Power Quality Conditioner (UPQC) is proposed for installation between the grid-connected RSMs and EV charging stations. The structural layout of the proposed system, including the placement of the UPQC, is illustrated in Figure 1.

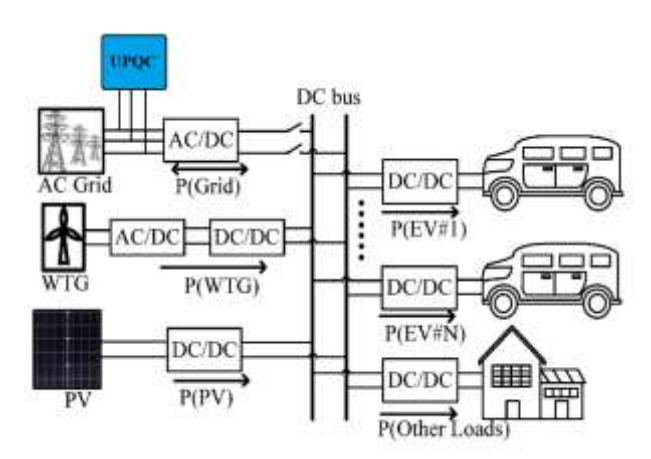


Figure 1 Outline structure of proposed system with UPQC

As observed in Figure 1 the grid is connected to an AC/DC converter with UPQC connected between the converter and the grid. The DC bus is connected to PV plant and Wind Turbine Generator (WTG) representing RSM. Multiple EV charging stations are connected to the same DC bus for consuming power from RSM and also the grid as per availability. Along with the EV charging stations general domestic/residential loads connected [17] [18]. The voltages sags and swells introduced on the grid side and the harmonics generated by the RSM and EV charging station are mitigated by the UPQC connected at the intersection. Each module has their individual power circuit with individual controller for stabilizing the voltage of the devices. The UPQC receives feedback from the AC/DC converter current and the grid voltages for synchronized compensation [19] [20].

For optimal mitigation of voltage sags, swells and harmonics adaptive and hybrid regulators are adopted into UPQC controllers. The paper is organized with introduction to the proposed system with outline structure of grid connected RSM, EV charging station and UPQC in section 1. The introduction section represents the modules used in the proposed system with placement location. The following section 2 has the design and structure of the RSM and EV charging station connected at the DC bus of the system. In section 3 the modeling and design of UPQC and controllers of the series and shunt converters are discussed. The further updated of the adaptive and hybrid regulators introduced into the series and shunt controllers is presented in section 4. The final section 5 has the conclusion to the paper presenting the possible generation of comparative results with different regulators in the controllers followed by references cited in the paper.

2. Rsm and ev charging station design

The RSMs considered for grid integration to reduce reliance on conventional power generation units include PV plants and WTGs. These two RSMs are regarded as the most reliable and efficient among available renewable energy sources. Given the abundance of solar irradiation and wind resources, they enable effective and sustainable power generation.

2.1 PV Plant RSM

The PV plant RSM consists of multiple solar cells grouped into panels, which are configured in series and parallel arrays to meet the desired power and voltage levels [21]–[24]. These interconnected PV panels are then connected to a boost power converter, which serves to regulate and stabilize the output voltage from the PV array. The internal structure of the PV plant RSM, including the boost converter, is illustrated in Figure 2.

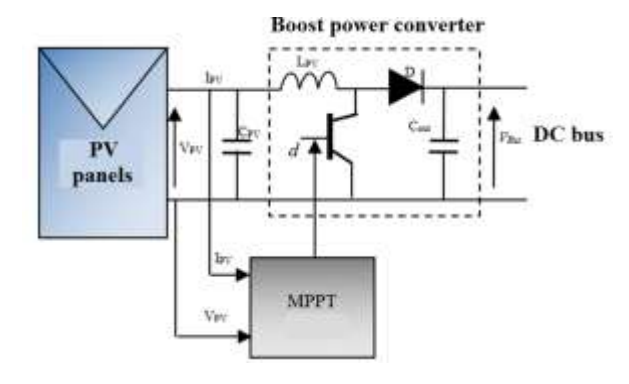


Figure 2 PV plant RSM with boost power converter

As shown in Figure 2, the boost power converter switch—typically an IGBT—is controlled by a

Maximum Power Point Tracking (MPPT) controller. This controller receives real-time voltage and current feedback from the PV panels. Various MPPT techniques are available for extracting the maximum possible power from the PV system, including Observe (P&O), Perturb and Incremental Conductance, Hill Climbing, and Fuzzy Logic-based methods [25]-[29]. The speed and accuracy of the MPPT algorithm directly affect how quickly the boost converter can respond to environmental changes and stabilize the output voltage. The regulated output of the boost converter is connected to a DC bus, facilitating power sharing from the PV plant RSM. The WTG RSM consists of a wind propeller, turbine, and generator, all mechanically coupled through a series of gear systems. Wind flow rotates the large propeller, which, via the gear mechanism, drives the turbine at higher rotational speeds [30]–[33]. The turbine shaft is mechanically connected to a generator, converting mechanical energy into electrical energy. In standalone WTG systems, a PMSG is commonly used. As its name implies, the rotor of the PMSG contains permanent magnets and is driven by the turbine. The rotation of the magnetic rotor induces current in the stator windings, generating voltage [34]-[36]. The structural layout of a PMSG-based WTG RSM is illustrated in Figure 3.

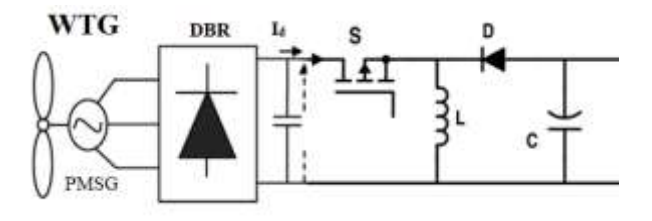


Figure 3 PMSG based WTG RSM

The WTG RSM, integrated with a PMSG, is connected to a Diode Bridge Rectifier (DBR) that converts the unpredictable and fluctuating AC output into a variable DC voltage. This variable DC voltage is then regulated using a unidirectional DC-DC **Buck-Boost** converter [37]-[38]. The converter's switching element, typically MOSFET, is controlled by an MPPT module, similar to the one used in the PV plant RSM. This configuration ensures that maximum power is extracted from the PMSG via the DBR and delivered efficiently through the Buck-Boost converter. Various MPPT strategies can be implemented for WTG systems, including Power Signal Feedback, Tip Speed Ratio (TSR) control, and Hill Climbing Search methods.

2.3 EV Charging Station

The EV charging station comprises multiple power conversion stages that adjust the DC bus voltage to levels suitable for charging EV batteries [39]–[42]. The primary converter used for battery charging is a DC-DC Buck converter, which is managed by dedicated control modules to ensure proper voltage and current regulation during charging. The configuration of the EV charging station, including the Buck converters connected to the EV battery, is shown in Figure 4

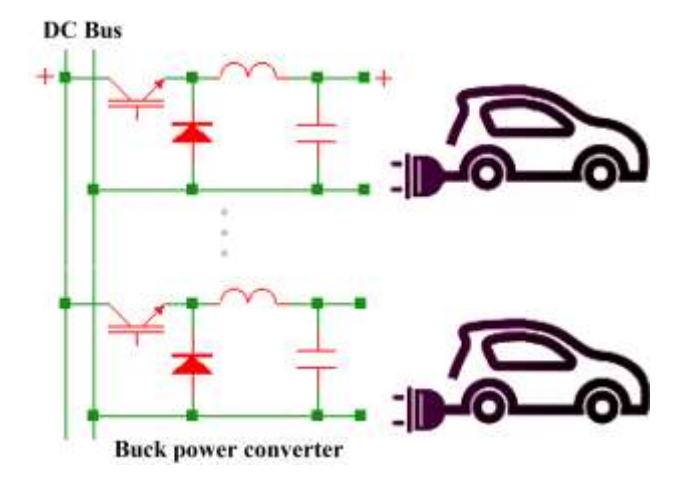


Figure 4 EV charging station

Each Buck power converter used in the EV charging station includes an IGBT switch that operates under either Constant Current (CC) or Constant Voltage (CV) control modes, depending on the State of Charge (SOC) of the EV battery. The converter controller receives real-time feedback from the battery's voltage and current sensors. In CC mode, the controller regulates the current based on a reference current value, while in CV mode, it regulates the voltage based on a reference voltage. Typically, CC mode is engaged when the battery SOC is low, and CV mode is activated once the SOC exceeds a predefined threshold [43], [44]. This mode-switching strategy helps optimize battery life, improve reliability, and maintain long-term battery health.All modules connected to the DC bus interface with a common AC/DC converter, which facilitates power exchange between the grid and the DC bus. This converter is a six-switch topology controlled by a Synchronous Reference Frame (SRF) controller. The SRF controller ensures that the DC bus voltage remains stable at a predefined reference value [45]–[48]. The SRF controller operates in synchronization with the grid voltages to facilitate efficient power exchange between the DC bus and the grid [49]-[51]. When the power generated by the RSMs is insufficient to meet the demands of the EV charging station and connected loads, the AC/DC converter supplies the required power from the grid.

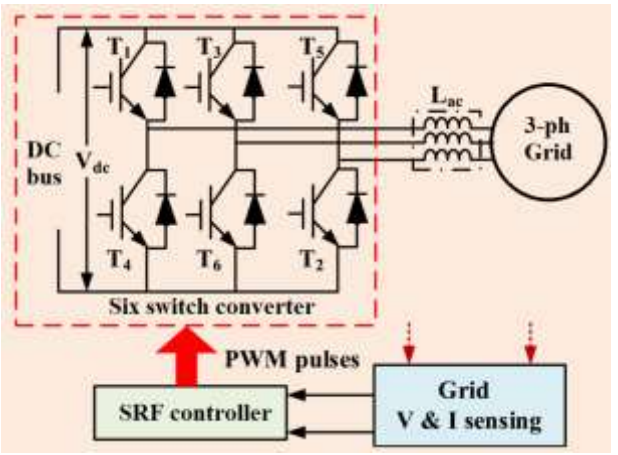


Figure 5 Grid connected six switch converters

Conversely, when the RSMs produce excess power beyond the consumption needs of the EV charging station and loads, the surplus energy is fed back into the grid through the same AC/DC converter. However, the six-switch AC/DC converter introduces harmonic distortions into the grid. To mitigate these power quality issues, a UPQC is installed at the interface between the grid and the six-switch converter shown in Figure 5 Grid connected six switch converters

3. UPQC Design

The UPQC is a type of Flexible AC Transmission System (FACTS) device designed to stabilize load-side voltages and simultaneously mitigate harmonics [52]–[56]. The UPQC consists of two power electronic converters: a series converter connected on the grid side and a shunt converter connected on the AC/DC converter side. Both converters use a six-switch, three-leg topology. These converters are interconnected back-to-back via a DC link capacitor (C_{DC}), which enables the exchange of energy between them in the form of voltage and current [57]–[61]. The structural configuration of the UPQC, placed at the interface between the grid and the AC/DC converter, is shown in Figure 6

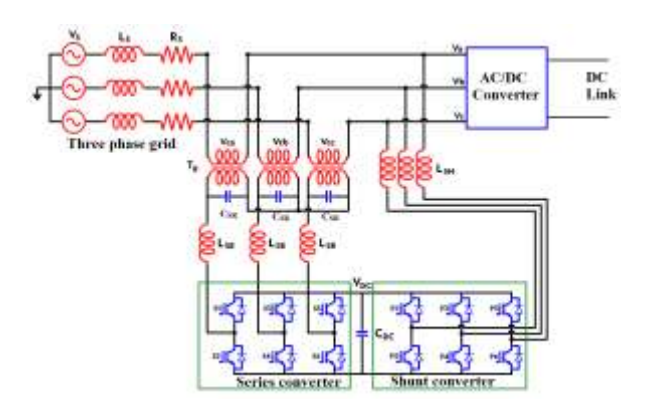


Figure 6 UPQC structure connected to AC/DC converter

As presented in Figure 6 the series converter is connected in series between the grid and AC/DC converter through series transformers (T_R). The series converter is connected to the series (L_{SR}) transformer through inductances and capacitors (C_{SR}) representing LC filter for harmonic elimination. However, the shunt converter is connected in parallel to the line through only inductors (L_{SH}) on the AC/DC converter side [62] – [65]. The series and shunt converters are operated by individual controller modules which operate as per the requirement. The Figure 7 are the series and shunt converter controller modules integrated in the UPQC device.

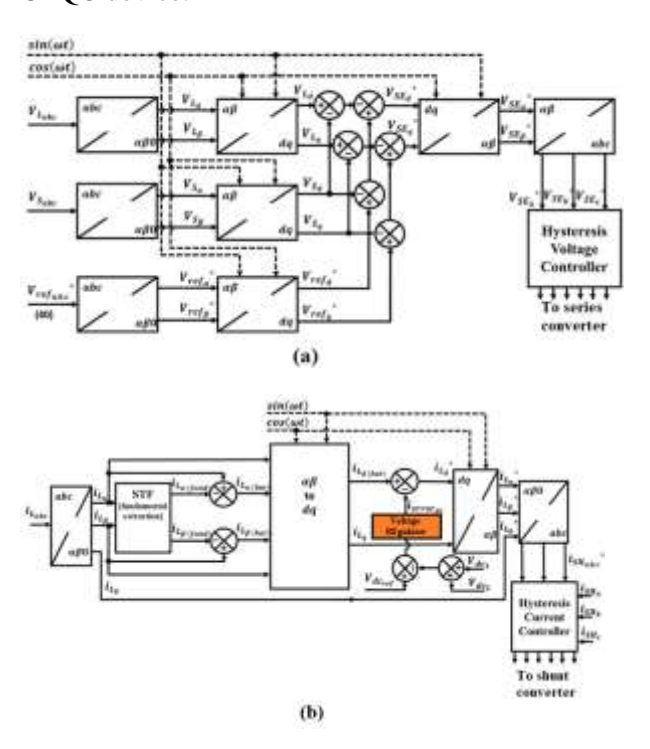


Figure 7 (a) Series controller (b) Shunt controller

As illustrated in Figures 7(a) and 7(b), the series controller does not include a voltage regulator, whereas the shunt controller is equipped with a voltage regulator. The primary function of the series

controller is to estimate the reference voltage V_{SE}* which represents the required voltage to be injected by the series converter. The pulse signals for the series converter are generated using a Hysteresis Voltage Controller.In contrast, the shunt controller contains a voltage regulator that calculates the current error (i_{error}) for harmonic compensation. This current error is used to determine the reference compensation currents (I_{SH}*) which are then utilized by the Hysteresis Current Controller to generate the gate pulses for the shunt converter [66]-[68]. Incorporating an optimal voltage regulator in the shunt converter significantly enhances the overall performance of the UPQC, leading to improved operational parameters for all devices connected to the system.

4. Different Controller Regulators

A wide range of regulators are employed across various control modules for tasks such as speed regulation, current control, voltage stabilization, and torque management. Among these, the Proportional-Integral (PI) regulator is one of the most widely used due to its simplicity and effectiveness in linear and less complex control systems.

4.1 PI Regulator

The PI regulator is a conventional control mechanism that combines proportional and integral gains, which are tuned according to the dynamic response of the system [69]. It is commonly preferred for its simple structure and ease of implementation. However, the PI regulator has notable limitations, including high initial overshoot, increased steady-state ripple, susceptibility to disturbances, and slower settling times [70]. The internal block diagram of a standard PI regulator is shown in Figure 8.

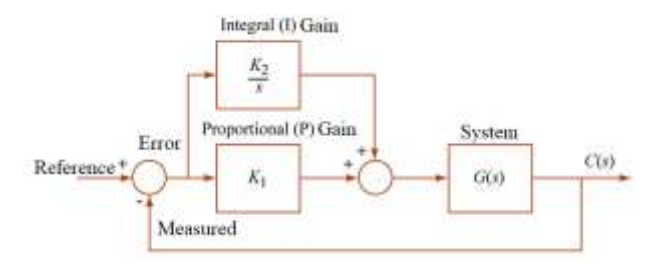


Figure 8 PI regulator internal structure

As presented in Figure 8, the proportional gain is addressed as K_1 and integral gain is addressed as K_2 . The input to the regulator is error signal generated by comparison of reference parameter with measured parameter. The parameters can be either current or voltage or speed as per the system's design [71]. The two gains are tuned using different

methods in which the 'trial and error' method is considered to be basic where the values are tuned as per the response of the system [72]. With the perfectly tuned values of K1 and K2 the controller operates optimally with reduced ripple, disturbances and oscillations.

4.2 AF-PI regulator

The PI regulator can further be updated with a 'Fuzzy Logic' design which can change the K_1 and K_2 values of the PI regulator making the regulator to work more extensively named to be AF-PI (Adaptive Fuzzy – PI) regulator [73] – [76]. The values of the K_1 and K_2 can be updated as per the 'error value' (e) and 'change in error value' (ce). As previously mentioned, the 'e' is generated by comparison of reference with measured parameter, the 'ce' value is generated by comparison of present 'e' with previous 'e' value [77].

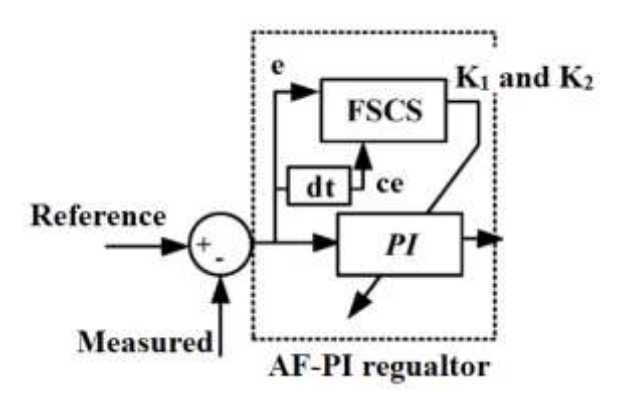


Figure 9 AF-PI regulator internal structure

The Figure 9 represents the structure of AF-PI regulator with PI regulator values K1 and K2 tuned by the FSCS (Fuzzy Set Control System) module. In the AF-PI regulator there are two sets of 'Fuzzy Logic' modules one for K_1 and other for K_2 gain generation. Each module comprises of two inputs (e and ce) and one output (K_1 or K_2) [78] – [81]. Each variable is set into several 'membership functions' (MFs) with different shapes set as per the requirement. The MFs of the input and output variables can be arranged as per given Figure 10

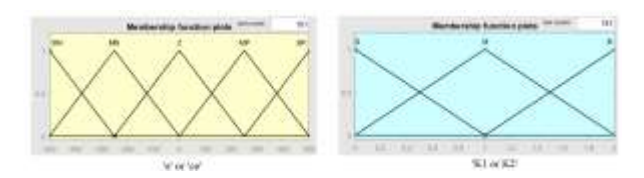


Figure 10 MFs of variables 'e' or 'ce' and 'o'

The input variable membership functions (MFs) are labelled as 'BN (Big Negative), MN (Medium Negative), Z (Zero), MP (Medium Positive), and BP (Big Positive)'. The output variable MFs are

categorized as 'S (Small), M (Medium), and B (Big)'. A similar MF structure is used for the gain ' K_2 ' as well. However, the variable ranges may differ depending on the plant's response. Each fuzzy design for the gains K_1 and K_2 is associated with its own set of 25 rules, detailed in Tables 1 and 2, respectively [82] [83].

Table 1: K_1 gain rule base

| 25 fuzzy rule base | | Variable 'e' | | | | | | |
|--------------------|----|--------------|----|---|----|----|--|--|
| | | BP | MP | Z | MN | BN | | |
| | BP | В | S | S | В | В | | |
| Variable | MP | В | В | S | В | В | | |
| 'ce' | Z | В | M | M | M | В | | |
| | MN | В | В | S | M | В | | |
| | BN | В | В | S | M | В | | |

Table 2: K_2 gain rule base

| 25 fuzzy rule base | | Variable 'e' | | | | | | |
|--------------------|----|--------------|----|---|----|----|--|--|
| | | BP | MP | Z | MN | BN | | |
| | BP | В | M | S | M | В | | |
| Variable | MP | В | M | M | M | В | | |
| 'ce' | Z | В | В | M | В | В | | |
| | MN | В | M | M | M | В | | |
| | BN | В | M | S | M | В | | |

As per the given rule base for each gain the output from the FSCS modules is updated to the PI controller for adaptive control on the gains for enhanced performance of the regulator impacting the system.

4.3 ANFIS regulator

The ANFIS (Adaptive Neuro Fuzzy Inference System) is an advanced regulator with data training using optimization technique. The ANFIS is a category of Fuzzy Logic module which involves 'Sugeno' type structure [84] [85]. Similar to the Fuzzy Logic module the ANFIS also has input and output variables. However, the input has only one variable 'e' and one output variable similar to PI regulator [86]. The MFs of the ANFIS regulator can be designed as presented in Figure 11

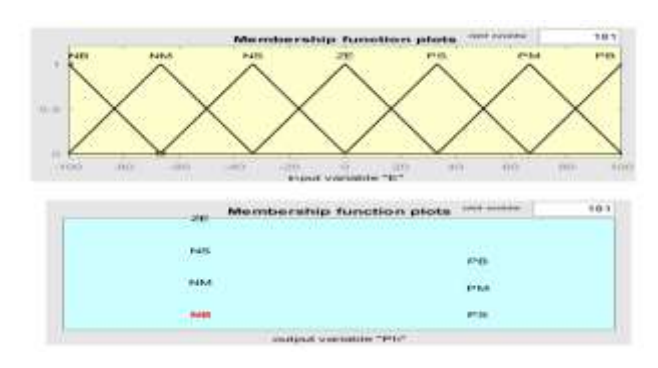


Figure 11 ANFIS variable MFs

The input variable 'e' is divided into seven membership functions (MFs), defined according to their position within a specified range. The MF centered at zero is labeled Zero (ZE). On the positive side of ZE, the MFs are named Positive Small (PS), Positive Medium (PM), and Positive Big (PB). Similarly, on the negative side, the MFs are defined as Negative Small (NS), Negative Medium (NM), and Negative Big (NB). The same set of seven MFs, with identical labels, is also used for the output variable of the ANFIS (Adaptive Neuro-Fuzzy Inference System) regulator [87]–[89]. The rule base for the ANFIS regulator consists of seven linear rules, each associating the corresponding input MF directly with the same output MF. Input-output data generated by the PI regulator is used to train the MFs within the ANFIS model. This training is performed using either the Backpropagation or Hybrid optimization algorithm, selected based on the controller's response to dynamic system changes [90], [91]. The results of the training process and the optimized rule base are illustrated in Figure 12.

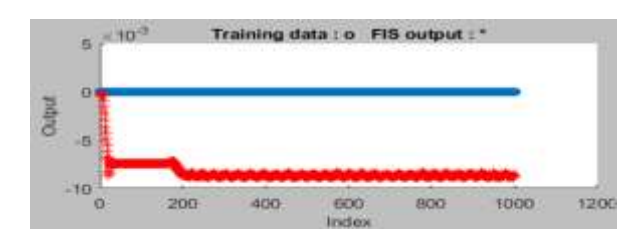


Figure 12 ANFIS trained data

The updated trained data with the optimization algorithm is updated to the regulator and the controller is upgraded to ANFIS based system. The performance of the converter is further tuned to operate more optimally with reduced disturbances.

4.4 SM - FOPI regulator

The Sliding Mode – Fractional Order PI (SM – FOPI) regulator is considered to be a hybrid regulator combining two regulators SMC (Sliding Mode Controller) and FOPI. This integration of both regulators creates more stability in the system with very less peak overshoots, ripple and oscillations [92] – [95]. The hybrid regulators are majorly used in system with higher transients and disturbances which operate adaptively as per the changes in the system. The Figure 13. represents the SM – FOPI regulator with one input and one output.

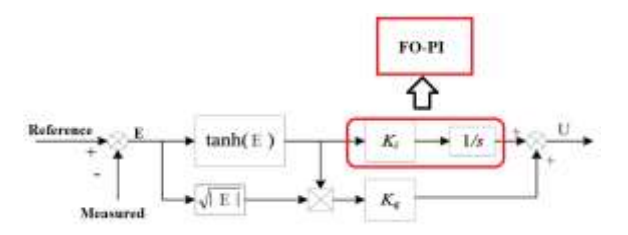


Figure 13 SM – FOPI regulator internal structure

As presented in the figure 13 the SMC with integral gain (K_i) is replaced by FO-PI regulator for better tuned value generation. Any higher oscillations in the error signal (E) due to sudden transient in the system is mitigated by the SMC and the required signal is further generated by the FO-PI regulator [96] - [99]. The FO-PI regulator also has two gains $(K_1$ and $K_2)$ similar to PI controller [100] - [102]. However, the integral is fractional order which generates less ripple reference signal. The internal structure of FO-PI regulator is presented in Figure 14

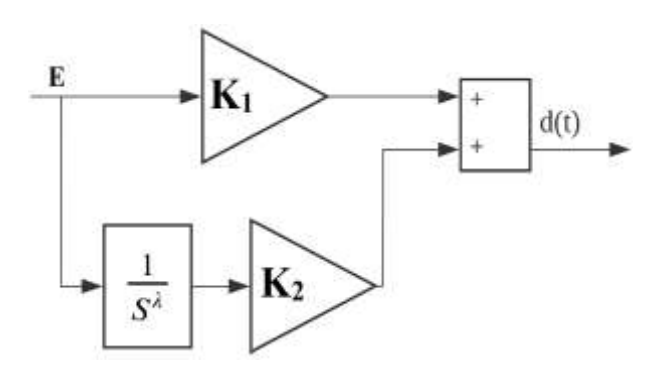


Figure 14 FO-PI regulator internal structure

As observed the integral has a superscript λ which is fractional and the value is between $(0 < \lambda < 1)$ [103] - [105]. The value can never be 0 or 1 as the regulator is fraction order. In most cases the SM-FOPI regulator operates with optimal signal generation with respect to the error signal (E).

5. Conclusion

This review paper presents a comprehensive description of a proposed system integrating renewable energy sources with an EV charging station, all connected via a common DC bus. The RSMs and the EV charging infrastructure, when interfaced with the grid through an AC/DC converter, introduce various power quality issues—such as harmonics, voltage sags, and swells—that must be addressed to ensure system reliability and performance. To mitigate these issues, a UPQC, a FACTS device comprising both series and shunt converters, is deployed at the interface between the grid and the AC/DC converter. The UPQC effectively compensates for harmonics and stabilizes

the voltage to maintain it within the desired standard limits. To further enhance the performance of the UPQC, various control regulators are incorporated into the controller module to generate precisely tuned reference signals. The use of adaptive and hybrid regulators helps to minimize disturbances, reduce ripple, and suppress transient overshoots in the reference signals. This paper briefly discusses the internal architectures of these regulators and outlines the overall system configuration and functionality.

Author Statements:

- **Ethical approval:** The conducted research is not related to either human or animal use.
- Conflict of interest: The authors declare that they have no known competing financial interests or personal relationships that could have appeared to influence the work reported in this paper
- Acknowledgement: The authors declare that they have nobody or no-company to acknowledge.
- **Author contributions:** The authors declare that they have equal right on this paper.
- **Funding information:** The authors declare that there is no funding to be acknowledged.
- **Data availability statement:** The data that support the findings of this study are available on request from the corresponding author. The data are not publicly available due to privacy or ethical restrictions.

References

- [1] Sansaniwal, S.K.; Sharma, V.; Mathur, J. Energy and exergy analyses of various typical solar energy applications: A comprehensive review. *Renew. Sustain. Energy Rev.* **2018**, 82, 1576–1601.
- [2] Islam, T.; Huda, N.; Abdullah, A.; Saidur, R. A comprehensive review of state-of-the-art concentrating solar power (CSP) technologies: Current status and research trends. *Renew. Sustain. Energy Rev.* **2018**, *91*, 987–1018.
- [3] Sultan, S.M.; Efzan, M.E. Review on recent Photovoltaic/Thermal (PV/T) technology advances and applications. *Sol. Energy* **2018**, *173*, 939–954.
- [4] Sumathi, S.; Ashok Kumar, L.; Surekha, P. Solar PV and Wind Energy Conversion Systems; Springer: Berlin/Heidelberg, Germany, 2015; ISBN 978-3-319-14940-0.
- [5] P. Silva, A. Cerveira and J. Baptista, "Impact of Electric Vehicle Charging Stations on Distribution Grids with PV Integration," 2023 International Conference on Electrical, Computer and Energy Technologies (ICECET), Cape Town, South Africa, 2023, pp. 1-6, doi: 10.1109/ICECET58911.2023.10389438.

- [6] D. Meyer and J. Wang, "Integrating ultra-fast charging stations within the power grids of smart cities: a review," IET Smart Grid, vol. 1, no. 1, pp. 3–10, 2018, doi: 10.1049/iet-stg.2018.0006.
- [7] "McKinsey Electric Vehicle Index: Europe cushions a global plunge in EV sales," McKinsey & Company, Jul. 2020. [Online]. Available: https://www.mckinsey.com/industries/automotive-and-assembly/our-insights/mckinsey-electric-vehicle-index-europe-cushions-a-global-plunge-inev-sales.
- [8] K. Knezovi'c, M. Marinelli, P. B. Andersen, and C. Træholt, "Concurrent provision of frequency regulation and overvoltage support by electric vehicles in a real Danish low voltage network," in 2014 IEEE International Electric Vehicle Conference (IEVC), Dec. 2014, pp. 1–7, doi: 10.1109/IEVC.2014.7056099.
- [9] M. E. Khodayar, L. Wu, and Z. Li, "Electric Vehicle Mobility in Transmission-Constrained Hourly Power Generation Scheduling," IEEE Trans. Smart Grid, vol. 4, no. 2, pp. 779–788, Jun. 2013, doi: 10.1109/TSG.2012.2230345.
- [10] X. Xi and R. Sioshansi, "Using Price-Based Signals to Control Plug-in Electric Vehicle Fleet Charging," IEEE Trans. Smart Grid, vol. 5, no. 3, pp. 1451– 1464, May 2014, doi: 10.1109/TSG.2014.2301931.
- [11] M. Alizadeh, H. Wai, A. Goldsmith, and A. Scaglione, "Retail and Wholesale Electricity Pricing Consider ing Electric Vehicle Mobility," IEEE Trans. Control Netw. Syst., vol. 6, no. 1, pp. 249–260, Mar. 2019, doi: 10.1109/TCNS.2018.2809960.
- [12] S. K. Khadem, M. Basu, and M. F. Conlon, "Intelligent islanding and seamless reconnection technique for microgrid with UPQC," IEEE J. Emerg. Sel. Topics Power Electron., vol. 3, no. 2, pp. 483–492, Jun. 2015.
- [13] J. M. Guerrero, P. C. Loh, T.-L. Lee, and M. Chandorkar, "Advanced control architectures for intelligent microgrids—Part II: Power quality, energy storage, and AC/DC microgrids," IEEE Trans. Ind. Electron., vol. 60, no. 4, pp. 1263–1270, Apr. 2013.
- [14] B. Han, B. Bae, H. Kim, and S. Baek, "Combined operation of unified power-quality conditioner with distributed generation," IEEE Trans. Power Del., vol. 21, no. 1, pp. 330–338, Jan. 2006.
- [15] K. Hasan, M. M. Othman, N. F. A. Rahman, M. A. Hannan, and I. Musirin, "Significant implication of unified power quality conditioner in power quality problems mitigation," Int. J. Power Electron. Drive Syst., vol. 10, no. 4, p. 2231, Dec. 2019.
- [16] C. K. Sundarabalan, Y. Puttagunta, and V. Vignesh, "Fuel cell integrated unified power quality conditioner for voltage and current reparation in four-wire distribution grid," IET Smart Grid, vol. 2, no. 1, pp. 60–68, Mar. 2019.
- [17] S. Devassy and B. Singh, "Design and performance analysis of three-phase solar PV integrated UPQC," IEEE Trans. Ind. Appl., vol. 54, no. 1, pp. 73–81, Jan. 2018.

- [18] L. B. G. Campanhol, S. A. O. da Silva, A. A. de Oliveira, and V. D. Bacon, "Power flow and stability analyses of a multifunctional distributed generation system integrating a photovoltaic system with unified power quality conditioner," IEEE Trans. Power Electron., vol. 34, no. 7, pp. 6241–6256, Jul. 2019.
- [19] A. M. Gee, F. Robinson, and W. Yuan, "A superconducting magnetic energy storage-emulator/battery supported dynamic voltage restorer," IEEE Trans. Energy Convers., vol. 32, no. 1, pp. 55–64, Mar. 2017.
- [20] W. U. Tareen and S. Mekhilef, "Transformer-less 3P3W SAPF (three-phase three-wire shunt active power filter) with line-interactive UPS (uninterruptible power supply) and battery energy storage stage," Energy, vol. 109, pp. 525–536, Aug. 2016.
- [21] L. Egiziano, N. Femia, D. Granozio, G. Petrone, G. Spagnuolo, and M. Vitelli, "Photovoltaic inverters with Perturb & Observe MPPT technique and one-cycle control," in Proc. IEEE Int. Symp. Circuits Syst., 2006, vol. 4, p. 3721.
- [22] N. Femia, G. Petrone, G. Spagnuolo, and M. Vitelli, "Optimization of Perturb and Observe maximum power point tracking method," IEEE Trans. Power. Electron., vol. 20, no. 4, pp. 963–973, Jul. 2005.
- [23] X. Liu and L. A. C. Lopes, "An improved perturbation and observation maximum power point tracking algorithm for PV arrays," in Proc. IEEE Power Electron. Spec. Conf., Jun. 2004, pp. 2005– 2010.
- [24] N. Femia, G. Petrone, G. Spagnuolo, and M. Vitelli, "Optimizing duty-cycle perturbation of P&O MPPT technique," in Proc. IEEE Power Electron. Spec. Conf., Jun. 2004, vol. 3, no. 1, pp. 1939–1944.
- [25] K.-H. Chao and C.-J. Li, "An intelligent maximum power point tracking method based on extension theory for PV systems," Expert Syst. Appl., vol. 37, no. 2, pp. 1050–1055, Mar. 2010.
- [26] F. Zhang, K. Thanapalan, J. Maddy, and A. Guwy, "Development of a novel hybrid maximum power point tracking methodology for photovoltaic systems," in Proc. IEEE Int. Conf. Autom. Comput., Sep. 2012, pp. 1–6.
- [27] N. Kasa, T. Iida, and G. Majumdar, "Robust control for maximum power point tracking in photovoltaic power system," in Proc. IEEE Power Con-vers. Conf., 2002, vol. 2, pp. 827–832.
- [28] D. P. Hohm and M. E. Ropp, "Comparative study of maximum power point tracking algorithms using an experimental, programmable, maximum power point tracking test," in Proc. IEEE Photovoltaic Spec. Conf., 2000, pp. 1699–1702.
- [29] K. Tse, M. Ho, H. S. H. Chung, and S. Hui, "A novel maximum power point tracker for PV panels using switching frequency modulation," IEEE Trans. Power. Electron., vol. 17, no. 6, pp. 980–989, Nov. 2002.
- [30] Fantino R, Solsona J, Busada C. Nonlinear observer-based control for PMSG wind turbine. Energy. 2016;113:248-257.

- [31] Jaramillo-Lopez F, Kenne G, Lamnabhi-Lagarrigue F. A novel online training neural network-based algorithm for wind speed estimation and adaptive control of PMSG wind turbine system for maximum power extraction. Renew Energy. 2016;86:38-48.
- [32] Errami Y, Ouassaid M, Maaroufi M. A performance comparison of a nonlinear and a linear control for grid connected PMSG wind energy conversion system. Int J Elec Power Energy Syst. 2015;68:180-194.
- [33] Matraji I, Al-Durra A, Errouissi R. Design and experimental validation of enhanced adaptive second-order SMC for PMSG-based wind energy conversion system. Int J Elec Power Energy Syst. 2018;103:21-30.
- [34] Abdelrahem, M.; Kennel, R. Fault-Ride through Strategy for Permanent-Magnet Synchronous Generators in Variable-Speed Wind Turbines. Energies 2016, 9, 1066.
- [35] Kim, K.; Jeung, Y.; Lee, D.; Kim, H. LVRT Scheme of PMSG Wind Power Systems Based on Feedback Linearization. IEEE Trans. Power Electron. 2012, 27, 2376–2384.
- [36] Nasiri, M.; Mobayen, S.; Zhu, Q.M. Super-Twisting Sliding Mode Control for Gearless PMSG-Based Wind Turbine. Complexity 2019, 2019, 6141607.
- [37] Pradhan, S.; Singh, B.; Panigrahi, B.K.; Murshid, S. A Composite Sliding Mode Controller for Wind Power Extraction in Remotely Located Solar PV—Wind Hybrid System. IEEE Trans. Ind. Electron. 2019, 66, 5321–5331.
- [38] Lee, S.-W.; Chun, K.-H. Adaptive Sliding Mode Control for PMSG Wind Turbine Systems. Energies 2019, 12, 595.
- [39] Neaimeha, M.; Salisbury, S.; Hill, G.; Blythe, P.; Scoffield, D.; Francfort, J. Analysing the usage and evidencing the importance of fast chargers for the adoption of battery electric vehicles. *Energy Policy* **2017**, *108*, 474–486.
- [40] Gnanna, T.; Funkea, S.; Jakobsson, N.; Plotza, P.; Sprei, F.; Bennehag, A. Fast charging infrastructure for electric vehicles: Today's situation and future needs. *Transp. Res. Part. D Transp. Environ.* **2018**, *62*, 314–329.
- [41] Kim, D.H.; Kim, M.S.; Nengroo, S.H.; Kim, C.H.; Kim, H.J. LLC Resonant Converter for LEV (Light Electric Vehicle) Fast Chargers. *Electronics* **2019**, *8*, 362.
- [42] Yan, X.; Li, J.; Zhang, B.; Jia, Z.; Tian, Y.; Zeng, H.; Lv, Z. Virtual Synchronous Motor Based-Control of a Three-Phase Electric Vehicle Off-Board Charger for Providing Fast-Charging Service. Appl. Sci. 2018, 8, 856.
- [43] Lia, J.; Wang, D.; Wang, W.; Jiang, J. Minimize Current Stress of Dual-Active-Bridge DC-DC Converters for Electric Vehicles Based on Lagrange Multipliers Method. *Energy Procedia* **2017**, *105*, 2733–2738.
- [44] Lee, I.; Lee, J. A High-Power DC-DC Converter Topology for Battery Charging Applications. *Energies* **2017**, *10*, 871.
- [45] F. Blaabjerg, R. RTeodorescu, M. Liserre, and A.V.Timbus, "Overview of Control and Grid

- Synchronization for Distributed Power Generation Systems," IEEE Trans. Ind. Electron., vol. 53, no. 5, pp 1398-1409, Oct. 2006.
- [46] E. Radziemska, and E.Klugmann "Photovoltaic Maximum Power Point Varying with Illumination and Temperature", in Journal of Solar Energy Engg., vol. 128, no. 1,pp.34-39
- [47] D. P. Hohm and M. E. Ropp, "Comparative Study of Maximum Power Point Tracking Algorithms", Progress in Photovoltaics: Research and Applications, 11, pp. 47-62, 2003.
- [48] Chia-Hsi Chang; Yu-Hui Lin; Yaow-Ming Chen; Yung Ruei Chang 'Simplified Reactive Power Control for Single-Phase Grid-Connected Photovoltaic Inverters' Industrial Electronics, IEEE Transactions on Volume: 61 Issue: 5, 2286 2296 .2014.
- [49] M. Liserre, R. Teodorescu, and F. Blaabjerg, "Stability of photovoltaic and wind turbine grid-connected inverters for a large set of grid impedance values," IEEE Trans. Power Electron., vol. 21, no. 1, pp. 263–272, Jan. 2006.
- [50] S. B. Kjaer, "Design and Control of an Inverter for Photovoltaic Applications," Ph.D. dissertation, Inst. Energy Technol., Aalborg University, Aalborg East, Denmark, 2004-2005.
- [51] Guan-Chyun Hsieh, and James C. Hung, "Phase-Locked Loop Techniques-A Survey," IEEE Trans. Ind. Electron., vol. 43, no. 6, pp 609-615, Dec. 1996.
- [52] P. Jayaprakash, B. Singh, D. Kothari, A. Chandra, and K. Al-Haddad, "Control of reduced-rating dynamic voltage restorer with a battery energy storage system," IEEE Trans. Ind. Appl., vol. 50, no. 2, pp. 1295–1303, Mar. 2014.
- [53] B. Singh, C. Jain, and S. Goel, "ILST control algorithm of single-stage dual purpose grid connected solar PV system," IEEE Trans. Power Electron., vol. 29, no. 10, pp. 5347–5357, Oct. 2014.
- [54] R. K. Agarwal, I. Hussain, and B. Singh, "Three-phase single-stage grid tied solar PV ECS using PLL-less fast CTF control technique," IET Power Electron., vol. 10, no. 2, pp. 178–188, 2017.
- [55] Y. Singh, I. Hussain, B. Singh, and S. Mishra, "Single-phase solar grid-interfaced system with active filtering using adaptive linear combiner filter-based control scheme," IET Gener., Transm. Distrib., vol. 11, no. 8, pp. 1976–1984, 2017.
- [56] T.-F. Wu, H.-S. Nien, C.-L. Shen, and T.-M. Chen, "A single-phase inverter system for PV power injection and active power filtering with nonlinear inductor consideration," IEEE Trans. Ind. Appl., vol. 41, no. 4, pp. 1075–1083, Jul. 2005.
- [57] A. Javadi, A. Hamadi, L. Woodward, and K. Al-Haddad, "Experimental investigation on a hybrid series active power compensator to improve power quality of typical households," IEEE Trans. Ind. Electron., vol. 63, no. 8, pp. 4849–4859, Aug. 2016.
- [58] A. Javadi, L. Woodward, and K. Al-Haddad, "Real-time implementation of a three-phase THSeAF based on VSC and p+r controller to improve power quality of weak distribution systems," in IEEE Trans. Power Electron., 2017, to be published, doi: 10.1109/TPEL.2017.2697821.

- [59] A. M. Rauf and V. Khadkikar, "Integrated photovoltaic and dynamic voltage restorer system configuration," IEEE Trans. Sustain. Energy,vol.6, no. 2, pp. 400–410, Apr. 2015.
- [60] S. Devassy and B. Singh, "Design and performance analysis of three-phase solar PV integrated UPQC," in Proc. 2016 IEEE 6th Int. Conf. Power Syst., Mar. 2016, pp. 1–6.
- [61] K. Palanisamy, D. Kothari, M. K. Mishra, S. Meikandashivam, and I.J. Raglend, "Effective utilization of unified power quality conditioner for interconnecting PV modules with grid using power angle control method," Int. J. Elect. Power Energy Syst., vol. 48, pp. 131–138, 2013.
- [63] S. Devassy and B. Singh, "Modified p-q theory based control of solar PV integrated UPQC-S," in IEEE Trans. Ind. Appl., vol. 53, no. 5, pp. 5031–5040, Sept./Oct. 2017, doi: 10.1109/TIA.2017.2714138.
- [64] S. K. Khadem, M. Basu, and M. F. Conlon, "Intelligent islanding and seamless reconnection technique for microgrid with UPQC," IEEE J. Emerg. Sel. Topics Power Electron., vol. 3, no. 2, pp. 483–492, Jun. 2015.
- [65] J. M. Guerrero, P. C. Loh, T. L. Lee, and M. Chandorkar, "Advanced control architectures for intelligent microgrids; Part II: Power quality, energy storage, and ac/dc microgrids," IEEE Trans. Ind. Electron., vol. 60, no. 4, pp. 1263–1270, Apr. 2013.
- [66] B. Singh and J. Solanki, "A comparison of control algorithms for dstat-com," IEEE Trans. Ind. Electron., vol. 56, no. 7, pp. 2738–2745, Jul. 2009.
- [67] B. Singh, C. Jain, S. Goel, A. Chandra, and K. Al-Haddad, "A multifunctional grid-tied solar energy conversion system with ANF-based control approach," IEEE Trans. Ind. Appl., vol. 52, no. 5, pp. 3663–3672, Sep. 2016.
- [68] S. Golestan, M. Ramezani, J. M. Guerrero, and M. Monfared, "dq-frame cascaded delayed signal cancellation- based PLL: Analysis, design, and comparison with moving average filter-based PLL," IEEE Trans. Power Electron., vol. 30, no. 3, pp. 1618–1632, Mar. 2015.
- [69] Z. Liu, H. Su, S. Pan, "A new adaptive sliding mode control of uncertain nonlinear systems", Asian Journal of Control, vol. 16, no. 1, (2014), pp. 198— 208
- [70] Y. Shang, "Consensus recovery from intentional attacks in directed nonlinear multi-agent systems", International Journal of Nonlinear Sciences and Numerical Simulation, 2013, vol. 14, no. 6, pp. 355-361
- [71] F. Piltan, A. R. Salehi & Nasri B Sulaiman, "Design Artificial Robust Control of Second Order System Based on Adaptive Fuzzy Gain Scheduling", World Applied Science Journal (WASJ), vol. 13, no. 5, (2011), pp. 1085-1092.
- [72] M. N. Kamarudin, A. R. Husain, M. N. Ahmad, "Control of uncertain nonlinear systems using mixed nonlinear damping function and backstepping techniques", 2012 IEEE International Conference on Control Systems, Computing and Engineering, (2012); Malaysia.

- [73] F. Piltan, N. Sulaiman, S.Soltani, M. H. Marhaban & R. Ramli, "An Adaptive Sliding Surface Slope Adjustment in PD Sliding Mode Fuzzy Control For Robot Manipulator", International Journal of Control and Automation, vol. 4, no. 3, (2011), pp. 65-76.
- [74] A. Siahbazi, A. Barzegar, M. Vosoogh, A. M. Mirshekaran, S. Soltani, "Design Modified Sliding Mode Controller with Parallel Fuzzy Inference System Compensator to Control of Spherical Motor", IJISA, vol.6, no.3, (2014), pp.12-25.
- [75] Zhilei Yao, Lan Xiao, J.M. Guerrero, Improved control strategy for the three-phase grid-connected inverter, IET Renew. Power Gener. 9 (6) (2015) 587–592.
- [76] N.R. Tummuru, M.K. Mishra, S. Srinivas, An improved current controller for grid connected voltage source converter in microgrid applications, IEEE Trans. Sustain. Energy 6 (2) (2015) 595–605.
- [77] T. Ye, N. Dai, C.S. Lam, M.C. Wong, J.M. Guerrero, Analysis, design, and implementation of a quasiproportional-resonant controller for a multifunctional capacitive-coupling grid-connected inverter, IEEE Trans. Ind. Appl. 52 (5) (2016) 4269– 4280.
- [78] W. Al-Saedi, S.W. Lachowicz, D. Habibi, O. Bass, Power flow control in grid-connected microgrid operation using particle swarm optimization under variable load conditions, Int. J. Electr. Power Energy Syst. 49 (2013) 76–85.
- [79] P. Garcia, C.A. Garcia, L.M. Fernandez, F. Llorens, F. Jurado, ANFIS-based control of a grid-connected hybrid system integrating renewable energies, hydrogen and batteries, IEEE Trans. Ind. Inform. 10 (2) (2014) 1107–1117.
- [80] I. Sefa, N. Altin, S. Ozdemir, O. Kaplan, Fuzzy PI controlled inverter for grid interactive renewable energy systems, IET Renew. Power Gener. 9 (7) (2015) 729–738.
- [81] H.M. Hasanien, M. Matar, A fuzzy logic controller for autonomous operation of a voltage source converter-based distributed generation system, IEEE Trans. Smart Grid 6 (1) (2015) 158–165.
- [82] M.A. Hannan, Z.A. Ghani, A. Mohamed, M.N. Uddin, Real-time testing of a fuzzy-logic-controllerbased grid-connected photovoltaic inverter system, IEEE Trans. Ind. Appl. 51 (6) (2015) 4775–4784.
- [83] L.X. Wang, A Course in Fuzzy Systems and Control, Prentice-Hall, 1997.
- [84] S. Mohagheghi, R.G. Harley, G.K. Venayagamoorthy, Modified Takagi–Sugeno fuzzy logic based controllers for a static compensator in a multimachine power system, Proc. IEEE Industry Applications Conference (2004) 2637–2642.
- [85] Jang JS (1993) ANFIS: Adaptive-network-based fuzzy inference system. IEEE Trans Syst Man Cybern 23(3):665–685
- [86] Pham DT, Koc E, Ghanbarzadeh A, Otri S, Rahim S, Zaidi M (2006) The bees algorithm: a novel tool for complex optimisation problems. In: Proceedings of the conference on intelligent production machines and system. Cardiff, UK, pp 454–459

- [87] Sitii M (2004) Atomic force microscope probe based controlled pushing for nanotribological characterization. IEEE/ASME Trans Mechatron 9(2):343–349
- [88] Shoorehdeli MA, Teshnehlab M, Sedigh AK (2009) Training ANFIS as an identifier with intelligent hybrid stable learning algorithm based on particle swarm optimization and extended Kalman filter. Fuzzy Sets Syst 160:922–948
- [89] Chatterjee A, Watanabe K (2006) An optimized Takagi–Sugeno type neuro-fuzzy system for modeling robot manipulators. Neural Comput Appl 15(1):55–61
- [90] Zangeneh AZ, Mansouri M, Teshnehlab M, Sedigh AK (2011) Training ANFIS system with DE algorithm. In: Proceedings of the IEEE international workshop on advanced computational intelligence (IWACI). Wuhan, pp 308–314
- [91] Cus F, Balic J, Zuperl UJ (2009) Hybrid ANFIS-ants system based optimisation of turning parameters. J Achiev Mater Manuf Eng 36(1):79–86
- [92] M. Ezzat, A. Glumineau, and F. Plestan, "Sensorless high order sliding mode control of permanent magnet synchronous motor," in Proc. 11th Int. Workshop Variable Struct. Syst., Jun. 2010, pp. 233–238.
- [93] L. Yuan, F. Xiao, J.-Q. Shen, M.-L. Chen, Q.-M. Shi, and L. Quan-Feng, "Sensorless control of highpower interior permanent-magnet synchronous motor drives at very low speed," IET Electr. Power Appl., vol. 7, no. 3, pp. 199–206, Mar. 2013.
- [94] D. Liang, J. Li, and R. Qu, "Sensorless control of permanent magnet synchronous machine based on second-order sliding-mode observer with online resistance estimation," IEEE Trans. Ind. Appl., vol. 53, no. 4, pp. 3672–3682, Jul./Aug. 2017.
- [95] G. Ruyuan and D. Fujun, "Design of permanent magnet synchronous motor torque ring controller based on super-twisting sliding mode," (in Chinese), Micromotor, vol. 51, no. 2, pp. 52–68, 2018.
- [96] W. Dongling, Z. Chaohui, W. Feiyu, and S. Qiang, "Speed and torque control based on super-twisting sliding mode permanent magnet synchronous motor," (in Chinese), Motor Control Appl., vol. 44, no. 10, pp. 42–47, 2017.
- [97] M. Ezzat, A. Glumineau, and F. Plestan, "Sensorless speed control of a permanent magnet synchronous motor: High order sliding mode controller and sliding mode observer," Proc. IFAC, vol. 43, no. 14, pp. 1290–1295, 2010.
- [98] Y.-B. Sun, X. Yang, J.-K. Xia, and C.-Y. Wang, "Second order sliding mode control of PMLSM based on diagonalization method," (in Chinese), Proc. Chin. Soc. Elect. Eng., vol. 28, no. 12, pp. 124–128, 2008.
- [99] Y. Chen, B. M. Vinagre, and I. Podlubny, "Fractional Order Disturbance Observer for Robust Vibration Suppression," Nonlinear Dynamics, vol. 38, no. 1, pp. 355–367, Dec. 2004.
- [100] S. Cheng, S. Wang, Y. Wei, Q. Liang, and Y. Wang, "Study on four disturbance observers for FO-LTI

- systems," IEEE/CAA J. Autom. Sinica, vol. 3, no. 4, pp. 442–450, Oct. 2016.
- [101] S. Li, H. Liu, and S. Ding, "A speed control for a PMSM using finite-time feedback control and disturbance compensation," Trans. of the Institute of Measurement and Control, vol. 32, no. 2, pp. 170–187, 2010.
- [102] S. Li, M. Zhou, and X. Yu, "Design and implementation of terminal slidingmode control method for PMSM speed regulation system," IEEE Trans Ind. Informatics, vol. 9, no. 4, pp. 1879–1891, Nov. 2013.
- [103] S. Li, C. Xia, and X. Zhou, "Disturbance rejection control method for permanent magnet synchronous motor speed-regulation system," Mechatronics, Elsevier, vol. 22, pp. 706–714, Mar. 2012.
- [104] J. Yang, H. Liu, S. Li, and X. Chen, "Nonlinear disturbance observer based robust tracking control for a pmsm drive subject to mismatched uncertainties," in Proc. IEEE Chinese Control Conference, Jul. 2012, pp. 830–835.
- [105] P. Lino, G. Maione, S. Stasi, F. Padula, and A. Visioli, "Synthesis of fractional-order pi controllers and fractional-order filters for industrial electrical drives," IEEE/CAA J. Autom. Sinica, vol. 4, no. 1, pp. 58–69, Jan. 2017.